Brownian Dynamics with Hydrodynamic Interactions: The Application to Protein Diffusional Problems

By Eric Dickinson
PROCTER DEPARTMENT OF FOOD SCIENCE, UNIVERSITY OF LEEDS,
LEEDS, LS2 9JT

1 Introduction

What we now call the Brownian motion of microscopic particles was described for the first time in 1828 by the botanist Robert Brown.[1] Some sixty years later, Goüy correctly attributed[2] the phenomenon to the thermal motion of the surrounding liquid molecules. It was observed at an early stage[2,3] that Brownian movement is most lively with small particles in liquids of low viscosity, and that Brownian drift velocities are some 10^8 times smaller than typical molecular velocities. Roughly speaking, particles can be defined as Brownian if they are larger than normal solvent molecules (or ions), but still small enough to be perturbed appreciably by solvent molecular motion. This puts them in the colloidal size range (1 nm—1 µm).

This article is concerned with the behaviour of proteins viewed as small colloidal particles. What follows is a description of how certain aspects of protein dynamics can be treated theoretically as problems which are soluble with the help of a computer. To establish our frame of reference, let us begin by listing some biological processes where we might tentatively expect Brownian motion to be a significant factor: (i) protein adsorption at a cell surface; (ii) the encounter between enzyme and substrate molecules; (iii) the interaction of an antibody with an antigen; (iv) protein mobility in a membrane, or along a fibre; (v) biochemical assembly by monomer aggregation or polymerization; and (vi) protein unfolding and denaturation. The common element in these processes is a kinetic stage which is diffusion controlled; and it is this element which we wish to emphasize here.

In chemistry and biology, the complexities of macroscopic change are driven by two types of physical events: time-reversible ones, which obey the classical laws (Newton's equations of motion), and time-irreversible ones, which obey probabilistic laws having their origin ultimately in the Second Law of Thermodynamics.[4] Generally speaking, systems containing a small number of interacting objects are time reversible, and those containing a very large number are time irreversible. The dynamics of a few interacting Brownian particles immersed in an inert fluid medium (millions of molecules) can be regarded as being partly deterministic (reversible) and partly chaotic (irreversible). The deterministic part of the motion arises from interparticle colloidal forces (electrostatic, van der Waals, etc.) and the influence of external fields (magnetic, gravitational, etc.). The

[1] R. Brown, *Ann. d. Phys. u. Chem.*, 1828, **14**, 294.
[2] M. Goüy, *J. Physique (Paris)*, 1888, **7**, 561.
[3] F. M. Exner, *Ann. Phys.*, 1900, **2**, 843.
[4] I. Prigogine and I. Stengers, 'Order out of Chaos', Heinemann, London, 1984.

chaotic part of the motion is associated with fluctuating Brownian forces from the apparently random thermal motion of the solvent molecules. The random impacts of surrounding molecules also give rise to frictional forces acting on the particles. Since the size of these frictional forces is dependent on the relative separations of the particles, it is found that the Brownian motions of the different particles, whilst remaining irregular, are in fact statistically coupled *via* the fluid medium.

The description of condensed matter of interest here is one combining Brownian motion with continuum hydrodynamics. The subject of Brownian motion deals with such entities as *colloidal* particles, diffusion coefficients, and statistical probabilities; hydrodynamics, on the other hand, is concerned with *macroscopic* bodies, steady flow, and continuum dynamics. Bring the two together and, to coin a phrase, we get Brownian dynamics. This is a kinetic theory essentially diffusive in character, but also including the effects of particle interactions, both hydro-dynamical and colloidal. Brownian dynamics is appropriate for describing protein motions over distances which are large compared with the solvent molecular size, and times which are long compared with the interval between successive solvent impacts.

In practice, most Brownian dynamics problems of chemical interest are not amenable to analytic solutions, but can be solved numerically using a computer. The usefulness of computer simulation in describing the dynamics of proteins is becoming increasingly recognized,[5-7] if not quite yet universally accepted.[8] A great strength of simulation, sometimes called 'computer experiment', is that it enables one to follow the consequences of changing certain variables independently in a way not possible often in a real experiment. In outlining suitable models for protein simulation, we shall be concerned here with emphasizing the underlying physical features. Necessarily, this will be at the expense of omitting some of the biochemical ramifications—although, in principle, the approach is sufficiently general to include all detailed aspects if the time and trouble are taken to put them in.

2 Basic Principles

Although Brownian-dynamics computer simulation is a relatively new field of study, it is based on some old and well-established principles. We begin our discussion of the theoretical background by mentioning the major historical contributions.

A. Einstein's Equation.—In his classic paper on Brownian movement, published in 1905, Einstein showed[9] that the average displacement x_{av} of a tagged particle in one-dimensional projection follows equation 1

$$x_{av} = (\langle x^2 \rangle)^{\frac{1}{2}} = (2Dt)^{\frac{1}{2}} \tag{1}$$

[5] J. A. McCammon and M. Karplus, *Ann. Rev. Phys. Chem.*, 1980, **31**, 29.

[6] M. Karplus, *Ber. Bunsenges. Phys. Chem.*, 1982, **86**, 386.

[7] J. A. McCammon, *Rep. Prog. Phys.*, 1984, **47**, 1.

[8] A. Cooper, *Prog. Biophys. Molec. Biol.*, 1984, **44**, 181.

[9] A. Einstein, *Ann. Phys.*, 1905, **17**, 549 (English translation: 'Albert Einstein, Investigations on the Theory of Brownian Movement', ed. R. Fürth, Dover, New York, 1956). See also: A. Pais, '"Subtle is the Lord . . .", The Science and Life of Albert Einstein', Oxford University Press, New York, 1982, chap. 5.

where t is time, D is a diffusion coefficient, and $\langle x^2 \rangle$ is the mean-square displacement in the x-direction. As each cartesian direction is equivalent, it follows that

$$\langle r^2 \rangle = \langle x^2 \rangle + \langle y^2 \rangle + \langle z^2 \rangle = 3\langle x^2 \rangle \tag{2}$$

where r is the total instantaneous distance travelled by the particle in time t. The crux of the derivation of equation 1, set out briefly below, is the recognition that the time-dependent probability distribution for random movement of a single particle is mathematically equivalent to the development of the concentration profile in bulk diffusion.

Imagine a large number n of identical non-interacting* particles. They are accumulated at time $t = 0$ in the immediate vicinity of the plane at $x = 0$, and then left to themselves. The change in local particle density $\rho(x,t)$ at position x and time t is described by the differential equation

$$\partial\rho/\partial t = D(\partial^2\rho/\partial x^2) \tag{3}$$

known usually as Fick's Second Law of Diffusion.[10] The density profile is found by solving equation 3 subject to boundary conditions,

$$\rho(x,t) = 0, \quad \begin{cases} (x \neq 0, t = 0) \\ (x \to \pm\infty, t > 0) \end{cases} \tag{4}$$

and a normalization condition, equation 5.

$$\int_{-\infty}^{+\infty} \rho(x,t)\,\mathrm{d}x = n \tag{5}$$

As material has an equal chance of diffusing to the left $(-x)$ or right $(+x)$, the mean displacement $\langle x \rangle$ is obviously zero. The developing profile from equations 3—5 is a normal distribution centred at $x = 0$:

$$\rho(x,t) = n(4\pi Dt)^{-\frac{1}{2}} \exp\left(-x^2/4Dt\right) \tag{6}$$

Combining equation 6 with the definition of the mean-square displacement, equation 7,

$$\langle x^2 \rangle = n^{-1} \int_{-\infty}^{+\infty} \rho(x,t)x^2\,\mathrm{d}x \tag{7}$$

gives Einstein's equation (equation 1) after integration.

---

* All real particles do, of course, interact strongly at close range. The theoretical position can be realized in the laboratory, however, if we imagine that the particles are so widely distributed in the y–z plane that pairs have negligible chance of colliding during the time-scale of observation.

[10] A. E. Fick, *Philos. Mag.*, 1855, **10**, 30.

A weakness in Einstein's original derivation, pointed out by Fürth,[11] is the necessity to invoke a time interval τ which is small compared with t, but nevertheless of such magnitude that movements executed by a particle in two successive intervals τ are considered as mutually independent. When the time for particle motion is short, this assumption is no longer valid. Under these circumstances, $\langle x^2 \rangle$ is properly given by[11,12] equation 8

$$\langle x^2 \rangle = 2D[t - m\mu + \exp(-t/m\mu)] \tag{8}$$

where m is the particle mass, and μ is a coefficient of mobility defined below. Einstein's equation holds for $t \gg m\mu$. This lower limit of time validity increases with the square of the particle size (as $m \propto d^3$ and $\mu \propto d^{-1}$); it is *ca.* 10^{-7} s for a 1 μm neutrally-buoyant particle in water at room temperature.

B. Friction and Mobility Coefficients.—From chaotic Brownian motion, we now turn to the subject of steady hydrodynamic flow.[13]

When a small constant force F is applied to a macroscopic body immersed in a hydrodynamic fluid, it rapidly attains a constant velocity v given by

$$v = \mu F \tag{9}$$

where μ is a mobility coefficient. Under steady-state conditions, the applied force is exactly counterbalanced by a frictional force f:

$$F = -f = \zeta v \tag{10}$$

So the friction coefficient ζ is simply the reciprocal of μ. Both are related to the size and shape of the body, and the viscosity of the fluid, and the above equations provide the physical basis for determining macromolecular size and shape from techniques such as centrifugation or electrophoresis. Although strictly applicable only to objects in the macroscopic domain, there is a long history of successful application of hydrodynamic theory down to particles of the size of sucrose molecules.[13]

Whether one chooses to work in terms of friction or mobility coefficients is largely a matter of convenience. The distinction is trivial in equations 9 and 10, but more complicated for objects of arbitrary shape in the vicinity of other like objects. The magnitude of the friction (or mobility) coefficient then depends on the forces acting on *all* the objects immersed in the fluid, and mathematically this means that scalar quantities μ and ζ must be replaced by tensors $\mathbf{\mu}$ and $\mathbf{\zeta}$. Analogously, the scalar diffusion coefficient is replaced by a diffusion tensor $\mathbf{D}$.

C. Langevin's Equation.—The one-dimensional motion of an isolated Brownian

[11] R. Fürth, *Z. Phys.*, 1920, **2**, 244.
[12] L. S. Ornstein, *Proc. Amst.*, 1918, **21**, 96.
[13] J. Happel and H. Brenner, 'Low Reynolds Number Hydrodynamics', 2nd edn., Noordhoff, Leiden, 1973.

particle is described by the simple Langevin equation[14]

$$m(\mathrm{d}v/\mathrm{d}t) = -\zeta v + R(t) \tag{11}$$

where $R(t)$ represents a random force due to solvent collisions. Equation 11 is an example of a stochastic equation of motion. It is nothing more than Newton's equation of motion (mass $\times$ acceleration = force) plus a random term. The latter is normally assumed to satisfy two conditions: firstly, that the process $R(t)$ is Gaussian, and, secondly, that its correlation time is infinitely short, *i.e.*,

$$\langle R(t_1)R(t_2) \rangle = 2\pi G_c \delta(t_1 - t_2) \tag{12}$$

where t_1 and t_2 are two times, G_c is a constant, and $\delta(x)$ is the Dirac function [defined as $\int \delta(x)\mathrm{d}x = 1$ for $x = 0$, $\delta(x) = 0$ for $x \neq 0$]. It turns out that the Gaussian assumption holds for a particle of mass much larger than that of the solvent molecules, a condition which is readily satisfied for a globular protein in water.

The Langevin approach enables a link to be formed between a statistical quantity R and a hydrodynamic quantity ζ, leading to a formal expression for the diffusion coefficient (in velocity space) D_v:

$$m^2 D_v = \int_0^\infty \langle R(0)R(t) \rangle \, \mathrm{d}t = kT\zeta \tag{13}$$

From equations 12 and 13 we see that $G_c = (kT/\pi)\zeta$, and so the stochastic term is given by

$$\langle R(0)R(t) \rangle = 2kT\zeta\delta(t) \tag{14}$$

Equation 14 is one of the most fundamental relationships in statistical mechanics. Commonly known as the fluctuation–dissipation theorem,[15] it expresses a relationship between hydrodynamic dissipation and an ensemble average over fluctuations in the system. It is readily generalized to three dimensions, and the nature of the random force is independent of any systematic forces acting on the particles, whether they arise from interactions with other particles or from the influence of an external field. It also applies to rotational motion.[15]

3 Diffusion
A. Phenomenological Coefficients.—As applied to one-dimensional mass transport, Fick's First Law of Diffusion states[6] that the mass flux J_x in direction x is given by

[14] S. Chandrasekar, *Rev. Mod. Phys.*, 1943, **15**, 1 (reprinted in: 'Selected Papers on Noise and Stochastic Processes', ed. N. Wax, Dover, New York, 1959).
[15] R. Kubo, *Rep. Prog. Phys.*, 1966, **29**, 255. For rotational applications see: J. McConnell, 'Rotational Brownian Motion and Dielectric Theory', Academic Press, London, 1980.

$$J_x = -D(\partial\rho/\partial x) \tag{15}$$

where D is a phenomenological coefficient, and ρ is the local density of the diffusing species. In three dimensions, we have

$$\boldsymbol{J} = -D\nabla\rho \tag{16}$$

where ∇ is the del operator defined by

$$\nabla = \boldsymbol{i}(\partial/\partial x) + \boldsymbol{j}(\partial/\partial y) + \boldsymbol{k}(\partial/\partial z) \tag{17}$$

and $\boldsymbol{i}$, $\boldsymbol{j}$, and $\boldsymbol{k}$ are unit vectors in x, y, and z directions.

Consider a large number of identical particles far enough apart in a fluid that they do not interact in any way. Each particle requires six independent parameters $[q_i(i = 1,6)]$ to specify its instantaneous configuration. Three parameters define position (x,y,z), and three define orientation $(\varphi_x, \varphi_y, \varphi_z)$. When Fick's Law is generalized to position–orientation space, each diffusive flux J_i $(i = 1,6)$ is linearly related to each density gradient $(\partial\rho/\partial q_j)$ $(j = 1,6)$ by the phenomenological equation

$$J_i = -D_{ij}(\partial\rho/\partial q_j) \tag{18}$$

where D_{ij} is now an element in a 6×6 matrix called the *diffusion tensor*, and ρ is the instantaneous particle density in position–orientation space. We represent the change in particle position during a small time interval dt by the vector

$$d\boldsymbol{r} = \boldsymbol{i}dq_1 + \boldsymbol{j}dq_2 + \boldsymbol{k}dq_3 = \boldsymbol{i}dx + \boldsymbol{j}dy + \boldsymbol{k}dz \tag{19}$$

where dx, dy, and dz are the projections of the displacement vector onto the cartesian axes. Similarly, the change in orientation is represented by the vector *

$$d\boldsymbol{\varphi} = \boldsymbol{i}dq_4 + \boldsymbol{j}dq_5 + \boldsymbol{k}dq_6 = \boldsymbol{i}d\varphi_x + \boldsymbol{j}d\varphi_y + \boldsymbol{k}d\varphi_z \tag{20}$$

where $d\varphi_x$, $d\varphi_y$, and $d\varphi_z$ denote projections onto the cartesian axes. In the same way that D in equation 15 has a statistical interpretation in terms of the Einstein equation (equation 1), we shall find that each of the elements in the diffusion tensor $\boldsymbol{D}$ defined by equation 18 also has a statistical interpretation.

B. An Isolated Spherical Particle.—The simplest possible system consists of a single, hard, spherical particle immersed in a quiescent hydrodynamic medium. Let us suppose that, during some small but finite time interval, the co-ordinates of the particle centre have moved from (x, y, z) to $(x + \Delta x, y + \Delta y, z + \Delta z)$. In the absence of any external forces, the mean-square Brownian displacements in the three directions are given by

$$\langle(\Delta x)^2\rangle = \langle(\Delta y)^2\rangle = \langle(\Delta z)^2\rangle = 2D^T\Delta t \tag{21}$$

* Unlike $d\boldsymbol{r}$, $d\boldsymbol{\varphi}$ is a vector only for infinitesimal displacements.

where D^T is a scalar translational diffusion coefficient. For a sphere of radius a in a medium of Newtonian viscosity η, D^T is given by the well-known Stokes-Einstein equation

$$D^T = kT/\zeta^T = kT/6\pi\eta a \qquad (22)$$

where ζ^T is the translational friction coefficient. During the same time interval Δt, the Brownian sphere will also have rotated through angles $\Delta\varphi_x$, $\Delta\varphi_y$, and $\Delta\varphi_z$ about axes parallel to the x, y, and z directions, respectively. Mean-square displacements are given by

$$\langle(\Delta\varphi_x)^2\rangle = \langle(\Delta\varphi_y)^2\rangle = \langle(\Delta\varphi_z)^2\rangle = 2D^R\Delta t \qquad (23)$$

where D^R is the rotational diffusion coefficient:

$$D^R = kT/8\pi\eta a^3 \qquad (24)$$

Comparing equations 22 and 24, we see that rotational motion decreases much more strongly with increasing particle size than does translational motion.

In position–orientation space, the generalized Einstein equation has the form

$$\langle\Delta q_i\Delta q_j\rangle = 2D_{ij}\Delta t \qquad (25)$$

In matrix notation, the diffusion tensor $\boldsymbol{D} = [D_{ij}]$ for a single sphere has non-zero elements only along the leading diagonal, *i.e.*,

$$\boldsymbol{D} = \begin{bmatrix} D_{11} & D_{12} & D_{13} & D_{14} & D_{15} & D_{16} \\ D_{21} & D_{22} & D_{23} & D_{24} & D_{25} & D_{26} \\ D_{31} & D_{32} & D_{33} & D_{34} & D_{35} & D_{36} \\ D_{41} & D_{42} & D_{43} & D_{44} & D_{45} & D_{46} \\ D_{51} & D_{52} & D_{53} & D_{54} & D_{55} & D_{56} \\ D_{61} & D_{62} & D_{63} & D_{64} & D_{65} & D_{66} \end{bmatrix} = \begin{bmatrix} D^T & 0 & 0 & 0 & 0 & 0 \\ 0 & D^T & 0 & 0 & 0 & 0 \\ 0 & 0 & D^T & 0 & 0 & 0 \\ 0 & 0 & 0 & D^R & 0 & 0 \\ 0 & 0 & 0 & 0 & D^R & 0 \\ 0 & 0 & 0 & 0 & 0 & D^R \end{bmatrix} \qquad (26)$$

The off-diagonal elements are all zero because each of the three translational and three rotational degrees of freedom is completely independent for a single spherically-isotropic particle:

$$\langle\Delta r_i\Delta r_j\rangle = \langle\Delta r_i\Delta\varphi_j\rangle = \langle\Delta\varphi_i\Delta\varphi_j\rangle = 0 \quad (1 \leqslant i \neq j \leqslant 3) \qquad (27)$$

C. An Isolated Non-spherical Particle.—Irrespective of the shape of a particle, the diffusion matrix $[D_{ij}]$ is always symmetric and positive-definite (*i.e.*, $\boldsymbol{D} = \boldsymbol{D}\dagger$, where $\dagger$ denotes the matrix transpose).* The 6×6 diffusion matrix in position–orientation space can be partitioned into four 3×3 submatrices:

---

* A *symmetric* tensor (matrix) is a square matrix which is equal to its transpose. The *transpose* matrix is formed by interchanging rows and columns. A symmetric tensor $\boldsymbol{T}$ is *positive-definite* if $\boldsymbol{v} \cdot \boldsymbol{T} \cdot \boldsymbol{v} > 0$ for any non-zero vector $\boldsymbol{v}$. (See Appendix for summary of rules of tensor multiplication.)

$$D = \begin{bmatrix} D^t & D^{c\dagger} \\ D^c & D^r \end{bmatrix} \tag{28}$$

D^t is a (symmetric) translational diffusion tensor of the form:

$$D^t = \begin{bmatrix} D^t_{11} & D^t_{12} & D^t_{13} \\ D^t_{21} & D^t_{22} & D^t_{23} \\ D^t_{31} & D^t_{32} & D^t_{33} \end{bmatrix} \tag{29}$$

It describes the translational Brownian motion of some point P rigidly fixed in the particle according to the equation

$$\langle \Delta r_i \Delta r_j \rangle = 2D^{tP}_{ij}\Delta t \quad (i,j = 1,3) \tag{30}$$

where the superscript P on D^{tP}_{ij} now denotes the fact that, since a body rotates as it moves, the translational diffusion coefficient depends on the location of P. Analogously, the (symmetric) rotational diffusion tensor D^r governs the rotational Brownian motion according to

$$\langle \Delta \varphi_i \Delta \varphi_j \rangle = 2D^r_{ij}\Delta t \quad (i,j = 1,3) \tag{31}$$

And a coupling tensor D^c describes the correlation between translational and rotational displacements:

$$\langle \Delta \varphi_i \Delta r_j \rangle = 2D^{cP}_{ij}\Delta t \quad (i,j = 1,3) \tag{32}$$

Again the superscript P on D^{cP}_{ij} denotes a dependence of the tensor on the location of point P.

The values of D^t and D^c corresponding to two different points on the particle, P and Q, are related by[16]

$$D^{tQ} - D^{tP} = (D^{cP} \times r_{PQ}) - (r_{PQ} \times D^{cP}) - (r_{PQ} \times D^r \times r_{PQ}) \tag{33}$$

$$D^{cQ} - D^{cP} = D^r \times r_{PQ} \tag{34}$$

where r_{PQ} is the position vector from P to Q, and $\times$ represents the usual vector cross-product (see Appendix). Any rigid particle possesses a unique point O, its centre of diffusion, for which D^c is symmetric (*i.e.*, $D^{cO} = D^{cO\dagger}$). The exact location of O is given by

$$r_{QO} = [(\mathrm{Tr}D^r)I - D^r]^{-1} \cdot \epsilon : D^{cQ} \tag{35}$$

where $\mathrm{Tr}D^r$ represents the trace of tensor D^r (the sum of terms on the leading diagonal, *i.e.*, $D^r_{11} + D^r_{22} + D^r_{33}$). The quantity I in equation 35 is the unit tensor (identity matrix) defined by

$$I = \begin{bmatrix} 1 & 0 & 0 \\ 0 & 1 & 0 \\ 0 & 0 & 1 \end{bmatrix} \qquad (36)$$

The quantity ϵ is a totally antisymmetric third-rank tensor $(3 \times 3 \times 3)$ known as the Levi–Civita density; in matrix notation, ϵ_{ijk} is defined by $\epsilon_{123} = \epsilon_{312} = \epsilon_{231} = 1$, $\epsilon_{131} = \epsilon_{321} = \epsilon_{213} = -1$, and zero elsewhere.

For a particle that is spherically isotropic,* Brownian diffusion is completely described by just two scalar coefficients D^T and D^R:

$$D^{tO} = D^T I, \quad D^r = D^R I, \quad D^{cO} = 0 \qquad (37)$$

But, even for a sphere, we note that D^c vanishes only at the centre. Many globular proteins are roughly ellipsoidal in shape with diffusion tensors of the form:

$$D^{tO} = \begin{bmatrix} D_{11}^{tO} & 0 & 0 \\ 0 & D_{22}^{tO} & 0 \\ 0 & 0 & D_{33}^{tO} \end{bmatrix}, \quad D^r = \begin{bmatrix} D_{11}^{r} & 0 & 0 \\ 0 & D_{22}^{r} & 0 \\ 0 & 0 & D_{33}^{r} \end{bmatrix}, \quad D^{cO} = 0 \qquad (38)$$

As with spheres and ellipsoids, so for a large class of particle shapes: at the centre of diffusion, translational and rotational motions are uncoupled, with corresponding fluxes, J^t and J^r, given by

$$J^t = -D^{tO} \cdot (\partial\rho/\partial r), \quad J^r = -D^r \cdot (\partial\rho/\partial\varphi) \qquad (39)$$

A non-vanishing coupling tensor is associated with a screw-like behaviour of the diffusing particle. With biopolymers possessing helicoidal symmetry about a single axis (say the x-axis), the coupling of translational and rotational motions is described by a single scalar coefficient D^C defined by[16]

$$\langle \Delta x \Delta\varphi_x \rangle = \pm 2D^C \Delta t \qquad (40)$$

where the algebraic sign on the right of equation 40 depends on the handedness of the enantiomorph. Interesting academically, but apparently not biologically, is the class of isotropic helicoids,[16]

$$D^{tO} = D^T I, \quad D^r = D^R I, \quad D^{cO} = D^C I \qquad (41)$$

which includes the spherical isotropic particle as a special case $(D^C = 0)$.

D. A Spherical Particle Near a Plane Surface.—Moving from the unbounded fluid medium, let us now consider the case of a spherical Brownian particle near a solid plane wall. Making the spatial environment of the particle asymmetric has its effect

---

* In this special category of geometrical objects are the sphere and the five regular polyhedra (tetrahedron, cube, *etc.*).

[16] H. Brenner, *J. Colloid Interface Sci.*, 1967, **23**, 407.

on the diffusion tensor $\boldsymbol{D}$. If the x-axis passes through the particle centre O perpendicular to the surface (see Figure 1), diffusion in the x-direction is slower than in the y- or z-directions ($D_{11}^{t0} < D_{22}^{t0} = D_{33}^{t0}$), and depends on the distance l between O and the surface. At the same time, rotational diffusion about the x-axis is faster than rotational diffusion about the y- or z-axes ($D_{11}^{r} > D_{22}^{r} = D_{33}^{r}$). The origin of these differences lies in a spatially-dependent slowing down of diffusive motion, translational, and rotational, due to hydrodynamic forces between the surface of the colloidal particle and the boundary wall (*vide infra*). In crude physical terms, we might say that the particle moves slower than it would do in an unbounded fluid because some extra thermal driving energy has to be used to push fluid from (or pull fluid into) the region between the particle and the surface. This extra work against the fluid resistance becomes greater with decreasing separation l.
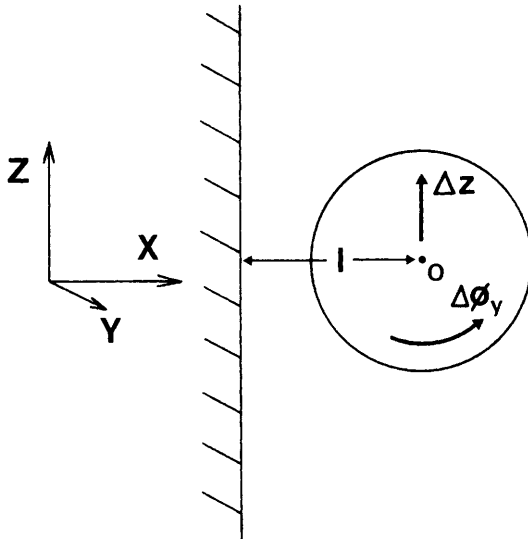

Figure 1 *Spherical particle with centre O at distance l from a plane surface. The translational displacement Δz is positively correlated with the rotational displacement $\Delta\varphi_y$*

With the isolated sphere, translational and rotational Brownian motion were completely independent (see equation 37). This is no longer the case in the presence of the surface. For example, a positional displacement Δz becomes positively correlated with an angular displacement $\Delta\varphi_y$, and the correlation is total in the limit of the sphere touching the plane ($l \to a$), when the particle can only move in a rolling motion. The single-particle diffusion tensor therefore has the following form:

$$D = \begin{bmatrix} D_{11} & 0 & 0 & 0 & 0 & 0 \\ 0 & D_{22} & 0 & 0 & 0 & D_{26} \\ 0 & 0 & D_{33} & 0 & D_{35} & 0 \\ 0 & 0 & 0 & D_{44} & 0 & 0 \\ 0 & 0 & D_{53} & 0 & D_{55} & 0 \\ 0 & D_{62} & 0 & 0 & 0 & D_{66} \end{bmatrix} \tag{42}$$

with $D_{22} = D_{33}, D_{55} = D_{66}, D_{26} = D_{62} = -D_{35} = -D_{53}$.

4 Hydrodynamics

In connection with the Brownian movement of small particles, we are nearly always concerned with hydrodynamics *at low Reynolds number*. That is to say, viscous forces from local shearing motions of the fluid are assumed to predominate over inertial forces associated with acceleration of the fluid elements. Strictly speaking, inertial forces exist to some small finite extent in all moving systems, but they can be neglected for the systems considered here.

A. Isolated Particles.—Frictional forces and torques exerted on a rigid macroscopic body are linearly related to translations and rotations by the friction tensor ζ. This 6 × 6 matrix can be decomposed into a 3 × 3 translational tensor ζ^t, a 3 × 3 rotational tensor ζ^r, and a 3 × 3 coupling tensor ζ^c:[17]

$$\zeta = \begin{bmatrix} \zeta^t & \zeta^{c\dagger} \\ \zeta^c & \zeta^r \end{bmatrix} \tag{43}$$

If we consider a point P on an isolated particle moving in an otherwise undisturbed fluid with rotational velocity ω and translational velocity v_P, the frictional force on the particle is given by

$$f = -\zeta^t \cdot v_P - \zeta^{cP\dagger} \cdot \omega \tag{44}$$

where as before the superscript P denotes a dependence on the location of P.* The frictional torque about P is given by

$$\tau_P = -\zeta^{cP} \cdot v_P - \zeta^{rP} \cdot \omega \tag{45}$$

where ζ^r, like ζ^c, is position-dependent. Every isolated rigid particle has a unique geometrical point, O, its centre of reaction, for which the coupling friction tensor is symmetric, *i.e.*,

$$\zeta^{cO} = \zeta^{cO\dagger} \tag{46}$$

---

* When the particle moves irrotationally, all points necessarily have the same translational velocity. As f is also independent of where P is located, this means that ζ^t has no position dependence. (Note the contrast here with D^t which is position-dependent.)

[17] H. Brenner, *Chem. Eng. Sci.*, 1964, **19**, 599.

But the centre of reaction is not necessarily located in the same place as the centre of diffusion.

At low Reynolds number, diffusion and friction tensors are related by a generalized Stokes–Einstein equation

$$D = kT\zeta^{-1} = kT\mu \tag{47}$$

where μ is the inverse of ζ. In terms of submatrices, we have:

$$\begin{bmatrix} D^{tP} & D^{cP\dagger} \\ D^{cP} & D^{r} \end{bmatrix} = kT \begin{bmatrix} \zeta^{t} & \zeta^{cP\dagger} \\ \zeta^{cP} & \zeta^{rP} \end{bmatrix}^{-1} = kT \begin{bmatrix} \mu^{tP} & \mu^{cP\dagger} \\ \mu^{cP} & \mu^{r} \end{bmatrix} \tag{48}$$

The individual components of D and ζ are related by[18]

$$D^{tP} = kT\{\zeta^{t} - [\zeta^{cP\dagger} \cdot (\zeta^{rP})^{-1} \cdot \zeta^{cP}]\}^{-1} \tag{49}$$

$$D^{r} = kT\{\zeta^{rP} - [\zeta^{cP} \cdot (\zeta^{t})^{-1} \cdot \zeta^{cP\dagger}]\}^{-1} \tag{50}$$

$$D^{cP} = -(\zeta^{rP})^{-1} \cdot \zeta^{cP} \cdot D^{tP} = -D^{r} \cdot \zeta^{cP} \cdot (\zeta^{t})^{-1} \tag{51}$$

We note in equation 51 that D^{c} and ζ^{c} vanish at the same location. For a nonskew particle ($\zeta^{cO} = 0$), the centres of diffusion and reaction coincide exactly. For screwlike particles ($\zeta^{cO} \neq 0$), it is shown by Wegener[18] that the centres of diffusion and reaction are generally in different places.

There are just two scalar friction coefficients for spherically isotropic particles:

$$\zeta^{t} = \zeta^{T}I, \quad \zeta^{rO} = \zeta^{R}I, \quad \zeta^{cO} = 0 \tag{52}$$

For a sphere of radius a, they take the simple form

$$\zeta^{T} = 6\pi\eta a, \quad \zeta^{R} = 8\pi\eta a^{3} \tag{53}$$

consistent with equations 22 and 24 for D^{T} and D^{R}. In practice, it is found that translation–rotation coupling effects for a single particle are not too important (less than a few per cent), so long as the object has some symmetry elements.[19] Only for highly asymmetric particles (*e.g.*, a half-turn of helix) is the effect very significant. With more than one particle, however, translation–rotation coupling is important even for spheres, as we shall see below.

B. Boundary Conditions: Stick *versus* Slip.—The Stokes formulae for the translational and rotational coefficients of a spherical particle (equation 53) are implicitly based on so-called 'stick' ('non-slip') boundary conditions. That is, the relative tangential velocity component of fluid in contact with the rigid particle surface is taken as zero. In practice, it is found that stick boundary conditions are correct for large, solid, and impermeable particles immersed in a viscous medium.

[18] W. A. Wegener, *Biopolymers*, 1981, **20**, 303.
[19] J. M. Garcia Bernal and J. Garcia de la Torre, *Biopolymers*, 1980, **19**, 751.

For a smooth spherical particle, at whose surface perfect slip occurs (*e.g.*, a gas bubble), the friction coefficients are given by

$$\zeta^T = 4\pi\eta a, \quad \zeta^R = 0 \tag{54}$$

For a liquid drop of finite viscosity η_i immersed in an unbounded continuum of viscosity η_0, the value of ζ^T lies between the pure slip and pure stick limits:

$$\zeta^T = 2\pi\eta a[(3 + (2\eta_0/\eta_i)][1 + (\eta_0/\eta_i)]^{-1} \tag{55}$$

In many real situations, the presence of surface-active agents makes the drop surface viscoelastic, in which case ζ^T and ζ^R approach the non-slip limits.[20]

Protein molecules are relatively small, non-spherical, flexible, and partly permeable to solvent; and so one might at first sight presume that rigid-sphere, stick boundary conditions would be out of the question. This is fortunately, however, not the case. In fact, the hydrodynamic properties of many protein molecules are adequately represented by effective hard-sphere models, and the roughness of the macromolecular surface usually means that stick boundary conditions are appropriate. Nevertheless, it needs to be pointed out that, as over half the water in contact with the protein surface is indistinguishable experimentally from pure solvent, it has been suggested[21] that a large proportion of the slip surface (*sic*) is between the vicinal water molecules and the protein, and not outside the first monolayer as commonly assumed.

Globular proteins are somewhat porous due to imperfect packing of subunits and topological surface irregularities. One possible way[22] of mimicing porosity is to relax partially the stick condition through a 'slipping length' defined by

$$v_t = \xi(\partial v_t/\partial n) \tag{56}$$

where v_t is the tangential velocity component, and $\partial v_t/\partial n$ is its derivative normal to the surface. The effective hydrodynamic radius a_{eff} of a sphere with this boundary condition is

$$a_{eff} = a[1 + 2(\xi/a)][1 + 3(\xi/a)]^{-1} \tag{57}$$

where $\xi \rightarrow \infty$ in the pure-slip limit (*cf.* $\eta_i = 0$ in equation 55). According to Wolynes and McCammon,[22] the ratio ξ/a is typically 0.15 for a porous protein.

Summarizing, then, we should treat stick boundary conditions as the norm, with full slip conditions only considered for species as small as solvent molecules, simple ions, or polymer segments.[23] Use of semi-empirical partial-slip boundary conditions has some intuitive appeal, but it is not rigorous except at a fluid–fluid interface. With solid particles, any relaxation of normal stick boundary conditions

[20] V. G. Levich, 'Physicochemical Hydrodynamics', Prentice-Hall, Englewood Cliffs, N.J., U.S.A., 1962.
[21] F. M. Richards, *Ann. Rev. Biophys. Bioeng.*, 1977, **6**, 151.
[22] P. G. Wolynes and J. A. McCammon, *Macromolecules*, 1977, **10**, 86.
[23] P. G. Wolynes and J. M. Deutch, *J. Chem. Phys.*, 1976, **65**, 450, 2030.

is really an admission that continuum hydrodynamic theory has broken down for the problem under investigation.

C. Hydrodynamic Interactions between Particles.—Consider two freely-rotating particles 1 and 2 acted on by forces F_1 and F_2 respectively. The particle velocities are given by

$$v_1 = \mu_{11}^t \cdot F_1 + \mu_{12}^t \cdot F_2 \tag{58}$$

$$v_2 = \mu_{21}^t \cdot F_1 + \mu_{22}^t \cdot F_2 \tag{59}$$

where μ_{ij}^t $(i,j = 1,2)$ are translational *pair* mobility tensors. The tensors μ_{11}^t and μ_{22}^t are equivalent to the single-particle tensors described above; μ_{12}^t and μ_{21}^t are new tensors arising specifically from the hydrodynamic pair interaction. For a pair of identical spheres with centres at separation r, the tensors have the general form

$$\mu_{ij}^t(r) = \alpha_{ij}^t(r) \, (rr/r^2) + \beta_{ij}^t(r) \, [I - (rr/r^2)] \tag{60}$$

where rr denotes the 3×3 dyad corresponding to vector r, and $\alpha_{ij}^t(r)$ and $\beta_{ij}^t(r)$ are scalar analytic functions of $r = |r|$. Mobility expressions are known[24] as a function of r to high accuracy with stick boundary conditions. The functions α^t and β^t can be expanded as series in powers of (a/r),[24] but at very close separations the series converge slowly and asymptotic expressions must be used instead.[13] The functions $\alpha_{ij}^t(r)$ and $\beta_{ij}^t(r)$ can be written explicitly in the form[25]

$$\alpha_{ij}^t(r) = (4\pi\eta a)^{-1} \sum_{n=0} a_n^{ij} \, (a/r)^{2n + |i - j|} \tag{61}$$

$$\beta_{ij}^t(r) = (4\pi\eta a)^{-1} \sum_{n=0} b_n^{ij} \, (a/r)^{2n + |i - j|} \tag{62}$$

Values of the expansion coefficients $[a_n^{11} \, (= a_n^{22}), \, a_n^{12} \, (= a_n^{21}), \, b_n^{11} \, (= b_n^{22})$ and $b_n^{12} \, (= b_n^{21})]$ are listed in Table 1 up to $n = 5$. The leading *self*-terms, a_0^{11} and b_0^{11}, are simply the reciprocals of the single-particle friction coefficients mentioned previously. Higher order *self*-terms represent the influence of the second particle on the single-particle friction coefficient of the first. Notice that some of the coefficients are exactly zero.

It is the *cross*-terms which are most important in Brownian kinetics, since these determine the relative motions of the diffusing species. Under stick boundary conditions, the leading *cross*-terms, a_0^{12} and b_0^{12}, combine to give what is commonly described in hydrodynamics as the Oseen tensor:[26]

$$D_{12}^t = kT\mu_{12}^t = (kT/8\pi\eta r)[I + (rr/r^2)] \tag{63}$$

[24] D. J. Jeffrey and Y. Onishi, *J. Fluid Mech.*, 1984, **139**, 261. R. Schmitz and B. U. Felderhof, *Physica*, 1982, **113A**, 90, 103; 1982, **116A**, 163.
[25] R. B. Jones and G. S. Burfield, *Physica*, 1985, **133A**, 152.
[26] C. W. Oseen, 'Hydrodynamik', Akademische Verlagsgellschaft, Leipzig, 1927.

Table 1 *Mobility expansion coefficients a_n^{ij} and b_n^{ij} ($n = 0,5$) for (A) stick and (B) slip boundary conditions*

| | a_n^{11} | | a_n^{12} | | b_n^{11} | | b_n^{12} | |
n	A	B	A	B	A	B	A	B
0	2/3	1	1	1	2/3	1	1/2	1/2
1	0	0	−2/3	0	0	0	1/3	0
2	−5/2	−1	0	0	0	0	0	0
3	11/3	−1	25/2	2	−17/24	1/8	0	0
4	7	−1	−5	6	−5/6	1/5	0	0
5	−167/3	−5	−131/2	14	−23/8	1/4	189/64	3/16

In the original derivation of equation 63, interacting elements were represented as point sources of friction; better approximations can be regarded as allowing for the effect of finite particle size on the hydrodynamic flow field. Extension of equation 63 to include expansion coefficients a_1^{12} and b_1^{12} leads to the equation of Rotne and Prager:[27]

$$D_{12}^t = (kT/8\pi\eta r)\{[I + (rr/r^2)] + (2a^2/3r^2)[I - 3(rr/r^2)]\} \qquad (64)$$

While the Rotne–Prager tensor is a better approximation than the Oseen tensor, both are unsatisfactory at close separations ($r \to 2a$). They overestimate the tendency of particles to move towards (or away from) one another along the line of centres; equation 63 is out by a factor of 10 for $r \sim 2.01a$. In the limit $r \to 2a$, the component * of D_{12}^t along the line of centres actually vanishes (the relative friction coefficient diverges to infinity). This means that, in the absence of colloidal attractive forces, perfectly hard spheres can never touch (coagulate) in a continuum solvent! The vanishing relative diffusion coefficient is due to very large velocity gradients in the gap between spheres with stick boundary conditions. The divergence in the friction coefficient with slip boundary conditions is much weaker, having the form of a logarithmic singularity.[23]

With more than two particles, things get more complicated, but the results can be expressed in a formally similar way. Mazur and van Saarloos have given[28] a general scheme for an arbitrary number of spheres to any order in (a/r). Explicit expressions to order $(a/r)^7$ are obtained for the mobility tensors, rotational as well as translational, and to this order three- and four-body interactions are included. The dominant contributions to translation from clusters of N spheres ($N \geqslant 2$) are of order $r^{-(3N-5)}$. As with the two-sphere case, certain powers of (a/r) are completely absent [*e.g.*, there is no term of order $(a/r)^5$ in the expression for μ^t].

D. Translation–Rotation Coupling.—When several bodies are immersed in a

---

* It is probably worthwhile emphasizing here that subscripts on D_{12}^t refer to particles 1 and 2, and not, as earlier (see equations 26 and 29), to directional components of the diffusion matrix.

[27] J. Rotne and S. Prager, *J. Chem. Phys.*, 1969, **50**, 4831.
[28] P. Mazur and W. van Saarloos, *Physica*, 1982, **115A**, 21.

hydrodynamic medium, the frictional forces and torques on each one of them depends on the translational and rotational movements of all the others. Generalizing equations 44 and 45 to an N-sphere system, the frictional force and torque on particle i is given by

$$f_i = -\sum_j^N (\zeta_{ij}^t \cdot v_j + \zeta_{ij}^c \cdot \omega_j) \tag{65}$$

$$\tau_i = -\sum_j^N (\zeta_{ij}^c \cdot v_j + \zeta_{ij}^r \cdot \omega_j) \tag{66}$$

where the superscripts t, c, and r denote hydrodynamic couplings between translation and translation, translation and rotation, and rotation and rotation, respectively. As with the single particle (equation 48), the combination of friction submatrices leads to a grand friction matrix related to grand mobility and diffusion matrices:[29]

$$\begin{bmatrix} D_{ij}^t & D_{ij}^c \\ D_{ij}^c & D_{ij}^r \end{bmatrix} = kT \begin{bmatrix} \mu_{ij}^t & \mu_{ij}^c \\ \mu_{ij}^c & \mu_{ij}^r \end{bmatrix} = kT \begin{bmatrix} \zeta_{ij}^t & \zeta_{ij}^c \\ \zeta_{ij}^c & \zeta_{ij}^r \end{bmatrix}^{-1} \tag{67}$$

Individual components of $[D_{ij}]$ and $[\zeta_{ij}]$ are related by sets of equations equivalent to those connecting the single-particle diffusion and friction tensors (equations 49—51).

The leading *cross*-terms in the diffusion tensor for a pair of rigid spheres are as follows:

$$D_{12}^t = (kT/8\pi\eta)r^{-1}[I + (rr/r^2)] + \mathcal{O}(r^{-3}) \tag{68}$$

$$D_{12}^c = -(kT/8\pi\eta)r^{-2}\varepsilon \cdot (r/r) + \mathcal{O}(r^{-8}) \tag{69}$$

$$D_{12}^r = (kT/16\pi\eta)r^{-3}[3(rr/r^2) - I] + \mathcal{O}(r^{-9}) \tag{70}$$

We note that interparticle translation–rotation coupling (equation 69) is of shorter range than rotation–rotation coupling (equation 70), but longer range than translation–rotation coupling (equation 68). With slip boundary conditions, the particles rotate freely, and so we have $D_{12}^c = D_{12}^r = 0$.

E. Particles Near a Plane Surface.—Since hydrodynamic interactions are of long range in comparison to particle size, the properties of particulate systems are strongly affected by boundary walls. The problem of one sphere in the vicinity of a plane surface is a limiting case of the two-sphere problem. It therefore provides a convenient system for testing the theories of hydrodynamic interaction in the laboratory. Recently, Ambari and co-workers have measured[30] the magnitude of the modified Stokes force f_x exerted on a macroscopic sphere ($a = 0.435$ mm) with centre O kept in magnetic levitation at a fixed distance l from the surface (see Figure

[29] D. W. Condiff and J. S. Dahler, *J. Chem. Phys.*, 1966, **44**, 3988.
[30] A. Ambari, B. Gauthier-Manuel, and E. Guyon, *J. Fluid Mech.*, 1984, **149**, 235.

2) using an optical feedback system. As the sphere approaches the wall with speed v_x, there is a change in frictional force given by

$$f_x = -6\pi\eta a v_x \delta(\varepsilon) \qquad (71)$$

where $\varepsilon a = l - a$ is the surface-to-surface separation. Within the experimental uncertainties, the data are found to agree exactly with theoretical equations derived for the cases of small[31] and large[32] separations:

$$\delta(\varepsilon) = \begin{cases} 1/\varepsilon - (\ln\varepsilon)/5 + 0.9712 + \ldots & (\varepsilon \to 0) \\ 1 + 9/8(1 + \varepsilon) + \ldots & (\varepsilon \gg 1) \end{cases} \qquad (72)$$

The expression for close separations comes from lubrication theory,[13] and the long-range formula is an Oseen-type representation. With the macroscopic sphere studied experimentally,[30] the smallest value of ε corresponded to a surface-to-surface separation of *ca.* 8 μm, well beyond the effective range of London/van der Waals attractive forces. (With particles of colloidal size, of course, this would not be the case.) At infinitesimally close separations, the frictional force diverges to infinity and the corresponding diffusion coefficient vanishes.
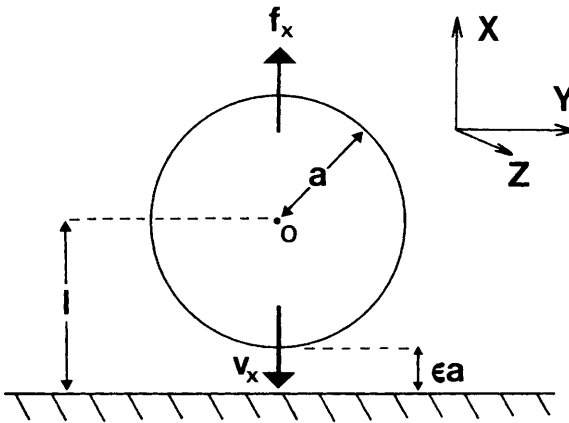

Figure 2 *Macroscopic sphere of radius* a *with centre* O *at distance* l *from a plane surface. As the sphere approaches the wall at speed* v_x, *it experiences a frictional force* f_x *at surface-to-surface separation* εa

There is less viscous resistance parallel to a plane wall than perpendicular to it. For a sphere moving parallel to a plane surface with stick boundary conditions, the frictional force f_y is related to the speed v_y by[33]

$$f_y = -6\pi\eta a v_y/[1 - (9a/16l) + (a/2l)^3 - \ldots] \qquad (73)$$

[31] R. G. Cox and H. Brenner, *Chem. Eng. Sci.*, 1967, **22**, 1753.
[32] H. A. Lorentz, *Abhandl. Theor. Phys.* (*Leipzig*), 1907, **1**, 23.
[33] H. Faxen, *Arkiv. Mat. Astron. Fys.*, 1923, **17**, No. 27.

The particle rotates with an angular velocity

$$\omega_z = (3v_y/32a)(a/l)^4 + \ldots \tag{74}$$

the direction being the same as that for simple rolling along the wall. We see from equation 74 that the strength of single-particle hydrodynamic translation–rotation coupling drops off rapidly with the particle–surface separation.

Expressions have recently been presented[34] for an arbitrary number of spheres in the vicinity of a plane wall. The main point to note is that, for the same surface-to-surface separation, the hydrodynamic effect of the wall is considerably greater than that of another spherical particle. And even more so for a cluster of particles between two plane walls.[13]

5 Brownian Dynamics Simulation
Just as the motion of atoms in a simple liquid can be simulated by molecular dynamics, the motion of particles in a colloidal dispersion can be computed numerically by Brownian dynamics. (In the purely hydrodynamic regime, where there is no Brownian movement, the term *Stokesian dynamics** seems appropriate.)

A. Algorithm of Ermak and McCammon.—In a system with colloidal inter-particle forces, the Langevin-type equation of translational motion has the form[35]

$$m_i(dv_i/dt) = -\sum_{j=1}^{3N} \zeta^t_{ij}v_j + F_i + \sum_{j=1}^{3N} \alpha^t_{ij}x_j \quad (i = 1, 3N) \tag{75}$$

where m_i is the particle mass associated with index i, v_i is the velocity component in direction i, F_i is the sum of external and interparticle forces acting in direction i, and the sum is over all $3N$ translational degrees of freedom (*cf.* the one-dimensional Langevin equation, equation 11). The right-hand-side of equation 75 is a sum of three terms: a frictional force, a systematic force, and a stochastic force. The stochastic term depends on a set of coefficients $\{\alpha^t_{ij}\}$, defined by

$$\zeta^t_{ij} = (kT)^{-1}\sum_k \alpha^t_{ik}\alpha^t_{jk} \tag{76}$$

and a set of random numbers $\{x_j\}$ with a Gaussian distribution,

$$\langle x_i(0)x_j(t)\rangle = 2\delta_{ij}\delta(t) \tag{77}$$

where δ_{ij} is the Kronecker delta ($= 1$ for $i = j$, otherwise zero).

---

* The author first heard this term used in public by Professor J. F. Brady at the Euromech symposium in Cambridge in April 1985 (see G. Bossis and J. F. Brady, *J. Chem. Phys.*, 1984, **80**, 5141).

[34] C. W. J. Beenakker, W. van Saarloos, and P. Mazur, *Physica*, 1984, **127A**, 451.

[35] J. M. Deutch and I. Oppenheim, *J. Chem. Phys.*, 1971, **54**, 3547.

A Brownian dynamics algorithm based on equations 75—77 was derived by Ermak and McCammon.[36] Particle displacements are given by

$$\Delta r_i = \sum_{j=1}^{3N} (\partial D_{ij}^{to}/\partial r_j)\Delta t + (kT)^{-1}\sum_{j=1}^{3N} D_{ij}^{to}F_j^0\Delta t + R_i(D_{ij}^{to},\Delta t), \ (i = 1,3N) \quad (78)$$

where $\Delta r = r_i - r_i^0$ is the change in particle co-ordinate during time-step Δt, R_i is the stochastic displacement in direction i, and superscript 0 denotes that the quantity is evaluated at the beginning of the step. It is important to note that in the algorithm defined by equation 78 instantaneous particle velocities are not specified as such. Although the interval Δt is long compared with the characteristic time associated with the solvent molecule motion, it must be short enough for quantities D_{ij}^{to} and F_j to be effectively constant during the simulation time-step. The stochastic displacements are calculated from the set of equations:

$$R_i(\Delta t) = \sum_{j=1}^{i} \sigma_{ij}X_j \quad (79)$$

$$\sigma_{ii} = \left[D_{ii}^{to} - \sum_{k=1}^{i-1}\sigma_{ik}^2 \right]^{\frac{1}{2}} \quad (80)$$

$$\sigma_{ij} = \sigma_{jj}^{-1}\left[D_{ij}^{to} - \sum_{k=1}^{j-1}\sigma_{ik}\sigma_{jk} \right] \ (i > j) \quad (81)$$

$$\langle X_i \rangle = 0, \qquad \langle X_iX_j \rangle = 2\delta_{ij}\Delta t \quad (82)$$

Because of the square root in equation 80, the calculation of σ_{ij} from D_{ij}^{to} is generally the most time-consuming part of the simulation.

The application of the algorithm of Ermak and McCammon to a particular problem requires specification of the configuration-dependent non-hydrodynamic forces $\{F_j\}$ associated with the various physico-chemical interactions between the Brownian particles. For instance, with electrostatically-stabilized colloidal particles, the contributions to $\{F_j\}$ come from derivatives of the DLVO potentials of mean force at the appropriate pair separations.[37] If a particle is also subject to an external force (*e.g.*, gravity), this is added in as well. A DLVO-type potential is suitable for describing the spherically-symmetric part of the protein–protein interaction, but there may also be asymmetric contributions to the protein potential arising, say, from highly charged, localized patches on the folded macromolecular surface. Once spherical symmetry is lost, particles are subject to torques as well as forces, which means that we must also consider the rotational Brownian motion (see next section).

There are some important technical differences between molecular dynamics and Brownian dynamics simulations. Molecular dynamics is based on Newton's equations of motion: energy is therefore conserved, and trajectories are time-reversible. On the other hand, a stochastic equation of motion like equation 78

[36] D. L. Ermak and J. A. McCammon, *J. Chem. Phys.*, 1978, **69**, 1352.
[37] J. Bacon, E. Dickinson, and R. Parker, *Faraday Discuss. Chem. Soc.*, 1983, **76**, 165. G. C. Ansell, E. Dickinson, and M. Ludvigsen, *J. Chem. Soc., Faraday Trans. 2*, 1985, **81**, 1269.

neither has a definite solution nor does it conserve energy. So, whereas total energy fluctuations can be used to monitor the efficacy of a molecular dynamics calculation, there is no such consistency check with Brownian dynamics. To ensure that particle trajectories are sufficiently accurate for the purpose in question, all one can do is demonstrate that average statistical properties are independent of the size of the integration time-step. In both types of simulation, contributions to forces $\{F_j\}$ can be truncated at pair separations beyond a certain 'cut-off' distance. However, in Brownian dynamics, because the hydrodynamic interactions are of long range, it is difficult to justify a particular 'cut-off' distance beyond which they may be neglected.

B. A Generalized Algorithm.—It is straightforward to generalize the above algorithm to include rotational Brownian motion and translational–rotation coupling. Proceeding along the lines of equations 65 and 66, one can write down a set of translational and rotational Langevin equations:[38]

$$m_i(dv_i/dt) = -\sum_{j=1}^{3N} \zeta_{ij}^{t}v_j - \sum_{j=3N+1}^{6N} \zeta_{ij}^{c}\omega_j + F_i + \sum_{j=1}^{6N} \alpha_{ij}x_j \quad (i = 1,3N) \qquad (83)$$

$$I_i(d\omega_i/dt) = -\sum_{j=1}^{3N} \zeta_{ij}^{c}v_j - \sum_{j=3N+1}^{6N} \zeta_{ij}^{r}\omega_j + T_i + \sum_{j=1}^{6N} \alpha_{ij}x_j \quad (i = 3N+1, 6N) \quad (84)$$

In equation 84, I_i is the moment of inertia associated with index i, and T_i is the sum of external and interparticle torques acting in direction i. The equations 83 and 84 are interdependent since they share the same set of α_{ij} coefficients defined by

$$\zeta_{ij} = (kT)^{-1}\sum_{k}\alpha_{ik}\alpha_{jk} \qquad (85)$$

Translational and rotational motions are only fully decoupled when $\zeta_{ij}^{c} = 0$ for all pairs of particles in the system.

Let us now switch to a set of generalized co-ordinates q_i ($i = 1,6N$) in $6N$-dimensional position–orientation space (see equations 19 and 20). Combining equations 83 and 84 into a single expression, we get a generalized Langevin equation from which can be derived[39] a generalized 'moving-on' routine:

$$\Delta q_i = \sum_{j=1}^{6N} (\partial D_{ij}^{0}/\partial q_j)\Delta t + (kT)^{-1} \sum_{j=1}^{6N} D_{ij}^{0}\mathscr{F}_j^{0}\Delta t + R_i(D_{ij}^{0},\Delta t) \quad (i = 1,6N) \qquad (86)$$

where $\Delta q_i = q_i - q_i^{0}$ is the change in generalized co-ordinate during Δt, and $\mathscr{F}_i$ is a generalized force component in direction i. Indices i and j from 1 to $3N$ refer to translation; those from $3N + 1$ to $6N$ to rotation. For spheres of uniform surface roughness, D_{ij} is independent of orientation, and so we have

[38] P. G. Wolynes and J. M. Deutch, *J. Chem. Phys.*, 1977, **67**, 733.
[39] E. Dickinson, S. A. Allison, and J. A. McCammon, *J. Chem. Soc., Faraday Trans.* 2, 1985, **81**, 591.

$$\partial D_{ij}/\partial q_j = 0 \quad (j = 3N+1, 6N) \tag{87}$$

In a system with rotational Brownian motion and translation–rotation coupling, the stochastic displacement terms are given by equations 79—82 as before, but $\boldsymbol{D}_{ij}^{to}$ is replaced by the grand diffusion tensor $\boldsymbol{D}_{ij}^{0}$.

C. Choice of Hydrodynamic Approximation.—A few words seem appropriate on the forms to be adopted for $\boldsymbol{\mu}_{ij}$ (and therefore $\boldsymbol{D}_{ij}$) in a simulation of spherical Brownian particles.

The Oseen and Rotne–Prager approximations, equations 63 and 64, are computationally convenient, but they break down at close separations ($r \rightarrow 2a$) where lubrication theory must be used. Fortunately, in many systems of realistically modelled Brownian particles, the problem is less severe than with simple hard spheres; this is because pairs of particles are in fact never allowed to get very close due to the influence of electrostatic interparticle repulsive forces. One disadvantage of crude pairwise-additive Oseen hydrodynamics is that it sometimes leads to a N-particle diffusion tensor that is not positive-definite. This is disastrous from the simulation standpoint, since it implies that the stochastic weightings from equations 79 and 80 are mathematically complex, and therefore physically absurd. One way round the difficulty is to use[39] a truncated Oseen interaction with $\mu_{12}^1 = 0$ for $r > r_c$, where the effective cut-off distance r_c is a decreasing function of the local particle concentration. The Rotne–Prager tensor is well-behaved, insofar as it does not suffer from non-positive-definiteness. And, like the Oseen tensor, it gives a computationally convenient divergenceless diffusion tensor ($\nabla \cdot \boldsymbol{D}_{ij}^1 = 0$), so that gradient terms in equations 78 and 86 need not be evaluated, thus saving some calculation time.

As mentioned previously, explicit expressions for $\boldsymbol{\mu}_{ij}$ are available[28] to order $(a/r)^7$, but their widespread use within Brownian dynamics simulations is likely to be restricted owing to the computational expense of having to sum over all groups of 3 and 4 particles for each time-step. In any case, recent calculations[40] cast doubt on whether in practice expressions to order $(a/r)^7$ give results in multi-particle systems that are any more reliable than those to order $(a/r)^3$ (Rotne–Prager approximation). One compromise solution[41] is to use an effective hydrodynamic pair tensor which allows for multi-body interactions implicitly *via* one or more empirical screening constants which depend on the local particle concentration. The idea here is that instead of having a sharp hydrodynamic cut-off,[37] one has a more gradual screening of the normal pair interaction. We note, however, that the concept of hydrodynamic screening is only strictly applicable to *immobile* particles immersed in a viscous medium.[42]

The justification for using simple hydrodynamic approximations in many Brownian dynamics problems comes from the fact that the rate processes are often only weakly affected by changes in the hydrodynamic expressions. Only when

[40] G. D. J. Phillies, *J. Chem. Phys.*, 1984, **81**, 4046.
[41] I. Snook, W. van Megen, and R. J. A. Tough, *J. Chem. Phys.*, 1983, **78**, 5825.
[42] C. W. J. Beenakker, *Faraday Discuss. Chem. Soc.*, 1983, **76**, 240.

particles spend most of their time very close together ($r - 2a \ll a$) does one need to be particularly careful about the exact form of the hydrodynamic interaction.[39]

6 Protein Dynamics

So much for the principles; now to the practice. Most of what follows is forward-looking: its aim is to point out what seems feasible in connection with the application of Brownian dynamics simulation to protein diffusional motion. In the case of the enzyme–substrate problem, some progress has already been made, but, for the most part, the field is still virgin territory. The topics described below are not meant to form a complete list. They just represent a few relevant and interesting problems about which the author has become recently aware. The unifying theme is Brownian dynamics with hydrodynamic interactions.

A. Enzyme–Substrate Encounters.—The enzyme–substrate combination is just one of several types of ligand–receptor pairs involved in biological action.[43] In the simplest possible model, enzyme and substrate molecules are represented as spherical Brownian particles with 'reactive patches' on parts of their surfaces. The overall rate of many biochemical processes is determined by the kinetics of an initial diffusional encounter between enzyme and substrate molecules, and the reaction is said to be 'diffusion controlled'. Amongst the factors that can affect the rate of reactive binary collision are the charge distributions on both molecules, the hydrodynamic interactions between the particles, the orientational dependence of reactivity, and intramolecular structural fluctuations at and near the 'active site'. Some limited progress has been made in incorporating these effects into analytic kinetic theories,[44] but it seems likely that the detailed distinguishing features of complicated biochemical processes will be amenable only to numerical simulation methods. An appealing feature of the simulation approach is the ability to make steady and systematic progress by successively refining the assumed model.

Let us consider the reaction sequence

$$E + S \underset{k'}{\overset{k}{\rightleftharpoons}} ES \xrightarrow{k''} \text{products} \qquad (88)$$
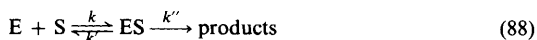
where E and S stand for enzyme and substrate respectively, and k, k' and k'' are rate constants. Under steady-state conditions ($d[ES]/dt = 0$), the transformation rate into products is described by an effective rate constant

$$k_{\text{eff}} = kk''/(k' + k'') \qquad (89)$$

We have $k_{\text{eff}} \approx k$ for a diffusion-controlled reaction ($k'' \gg k'$). When E and S are spherically-symmetric, non-interacting particles, the reaction is described by the bimolecular Smoluchowski rate constant[45]

$$k_{\text{s}} = 4\pi r_{\text{e}} D \qquad (90)$$

[43] J. A. McCammon, S. H. Northrup, and S. A. Allison, *Com. Molec. Cell. Biophys.*, in press.
[44] D. F. Calef and J. M. Deutch, *Ann. Rev. Phys. Chem.*, 1983, **34**, 493.
[45] M. V. Smoluchowski, *Phys. Z.*, 1916, **17**, 557.

where D is a diffusion coefficient, and r_e is an encounter distance (roughly equal to the sum of particle radii). Putting in some allowance for hydrodynamic effects, together with a general centrosymmetric potential of mean force $u(r)$ between E and S, leads to the modified Smoluchowski expression,[23,46]

$$k_s = 4\pi \left[\int_{r_e}^{\infty} r^{-2} [D(r)]^{-1} \exp[u(r)/kT] dr \right]^{-1} \qquad (91)$$

where D is now a function of the pair separation r (equivalent to the component of the pair diffusion tensor $\boldsymbol{D}_{12}^t$ along the line of centres).

Equation 91 represents more-or-less the limit of the analytic approach. When the E–S interaction is more complex than that assumed above, the rate constant must be evaluated numerically by averaging over diffusional trajectories of the substrate in the field of a fixed enzyme target.[43] To avoid having to simulate substrate paths which wander well away from the enzyme, the diffusion space around E is divided into two regions[47] (see Figure 3). In the outer region ($r > p$), E and S are far enough apart for diffusion to be described adequately by equation 91; in the inner region ($r \leqslant p$), however, interactions have a more complicated orientation dependence, and therefore must be handled numerically. If each Brownian collision of S with the active site on E leads to reaction, then it can be shown[47] that the rate constant is given by

$$k = k(p)\alpha\{1 - [(1 - \alpha)k(p)/k(q)]\}^{-1} \qquad (92)$$

where $k(p)$ and $k(q)$ are the values of k from equation 91 with $r_e = p$ and $r_e = q$, respectively. The quantity α represents the probability that a substrate molecule, starting at $r = p$, and free to diffuse in inner and outer regions, will react before reaching $r = q$. In the actual simulation, trajectories begin at $r = p$ and terminate on reaction or at $r = q$. From the fraction of events leading to reaction is calculated the bimolecular rate constant k. Detailed analysis of particle trajectories provides information about the reaction mechanism, *i.e.* whether or not S is 'steered' into productive collisional orientations during the diffusional encounter.

To take a particular example, McCammon and co-workers[48,49] have initiated a series of simulations of increasingly realistic models of the diffusion-controlled reaction of superoxide (O_2^-) catalysed by the enzyme superoxide dismutase. The enzyme molecule was represented as a sphere of diameter 6 nm having two small reactive patches on opposite sides covering *ca.* $1\frac{1}{2}\%$ of the total surface area. A set of five charges within the model enzyme particle was used to produce an electrostatic field with monopole, dipole, and quadrupole components equivalent to those generated by all 76 charged groups on the real protein. The O_2^- molecule is modelled as a sphere of diameter 0.3 nm carrying a unit charge. Rate constants

[46] S. H. Northrup and J. T. Hynes, *J. Chem. Phys.*, 1979, **71**, 871.
[47] S. H. Northrup, S. A. Allison, and J. A. McCammon, *J. Chem. Phys.*, 1984, **80**, 1517.
[48] S. A. Allison and J. A. McCammon, 1985, **89**, 1072.
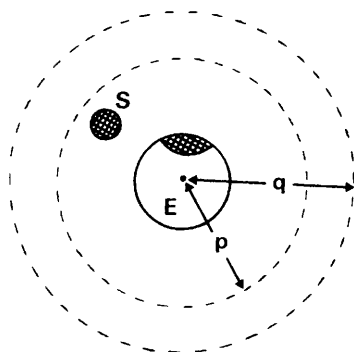[49] S. A. Allison, G. Ganti, and J. A. McCammon, *Biopolymers*, 1985, **24**, 1323.

Figure 3 *Simulation diffusion space for the encounter between enzyme E and substrate S. Distances* p *and* q *are the radii of the inner and outer diffusion regions (see text). The shaded portion of E denotes the 'active site'*

calculated from equation 92 were based on averages over several thousand trajectories with $p = 30$ nm and $q = 50$ nm, and the results were found to reproduce successfully the *qualitative* experimental features of the enzyme-catalysed reaction.[50] Using Debye–Hückel theory to allow for electrostatic screening, it is calculated in agreement with experiment that the rate constant first increases, and then decreases to a plateau, as the ionic strength is increased (*i.e.* as electrostatic interactions become of shorter effective range). It is postulated[43] that the initial increase in k is due to screening of long-range E–S repulsion, whereas the subsequent decrease arises from screening of the shorter-ranged non-central forces which act to steer the substrate into the active site.

The above results for O_2^- + superoxide dismutase refer to simulations in which hydrodynamic interactions were neglected altogether ($\boldsymbol{D}_{12} = 0$). Using the Oseen tensor with slip boundary conditions,* it has been shown[47] that including hydrodynamic interactions can lead to a reduction in simulated rate constant of *ca.* 30% in the absence of E–S attractive forces. In a separate Brownian dynamics simulation of encounters between a spherical enzyme particle and a dumbell-dimer substrate particle using a constraints algorithm (see later), it was found[52] that the presence of hydrodynamic interactions does not much affect the steering enhancements, but does lead to a fairly uniform decrease in the overall reaction rate. As the structural complexity of enzyme and substrate molecules increases, it is clear that the reaction kinetics is increasingly affected by orientational considerations, as determined by the rotational Brownian motion and (with stick boundary conditions) the coupling between translational and rotational motions.

* With a small substrate ion of solvent molecule dimensions, as is the case here, anything other than slip boundary conditions would seem inappropriate (see *ref.* 23 and 51).

[50] A. Cudd and I. Fridovich, *J. Biol. Chem.*, 1982, **257**, 11443. E. D. Getzoff, J. A. Tainer, P. K. Weiner, P. A. Zollman, J. S. Richardson, and D. C. Richardson, *Nature (London)*, 1983, **306**, 287.
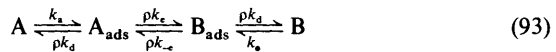
[51] R. Zwanzig and M. Bixon, *Phys. Rev. A*, 1970, **2**, 2002.

[52] S. A. Allison, N. Srinivasan, J. A. McCammon, and S. H. Northrup, *J. Phys. Chem.*, 1984, **88**, 6152.

B. Proteins at Electrode (and Related) Surfaces.—Protein electrochemistry offers the opportunity for controlled electronic communication with a wide range of biochemical processes. Using enzymes with redox-active sites, there is the possibility of converting electron movement into specific substrate transformations. The combination of immobilized glucose oxidase and a graphite electrode, for instance, has potential application in the amperometric determination of glucose in blood.[53]

Proteins appear to adsorb irreversibly at both synthetic and biological surfaces, and it has long been held the view that reversible electrochemistry involving proteins is not possible at conventional electrode surfaces. But, nevertheless, it is known[54] that reversible protein adsorption can occur if the protein is *rigid* and the surface is *hydrophilic*, conditions which ought to be fulfilled in many electrochemical situations involving redox proteins. In fact, recent work with cytochrome *c* at a gold electrode has shown[55] that 'good' electrochemistry is promoted in the presence of certain bifunctional organic compounds at the electrode surface. Cytochrome *c* is an example of a robust low-molecular-weight globular protein whose biochemical function is to carry electronic charge between the catalytic and energy transduction sites on the membrane of an organism. Efficient kinetics of electron transfer depends on the establishment of relatively long-lived, yet freely reversible, interactions of the protein, *in vivo* with its physiological redox partners, and *in vitro* with the electrode surface.

As a specific example, let us consider the conversion of *ferro*cytochrome *c* (A) to *ferri*cytochrome *c* (B) at a rotating disc electrode.[56] In the limit of fast mass transport, the reaction is represented by the scheme

$$A \underset{\rho k_d}{\overset{k_a}{\rightleftharpoons}} A_{ads} \underset{\rho k_{-e}}{\overset{\rho k_e}{\rightleftharpoons}} B_{ads} \underset{k_a}{\overset{\rho k_d}{\rightleftharpoons}} B \qquad (93)$$

where k_a is the rate of adsorption of reduced and oxidized forms, k_e and k_{-e} are the potential-dependent rate constants for the forward and backward electron-transfer reactions, k_d is the rate of desorption of reduced and oxidized forms, and ρ is the areal concentration of adsorption sites on the modified electrode. For reaction at a positive gold electrode ($k_e \gg k_{-e}$), values of the kinetic parameters are estimated[56] to be: $k_a = 3 \times 10^{-4}$ m s^{-1}, $k_e^0 = 50$ s^{-1}, $k_d = 50$ s^{-1}, and $\rho = 1.2$ mol m^{-2}. Reversible protein binding enhances the overall rate of the electrode reaction at the modified electrode, but the reaction is very slow at the unmodified electrode. The importance of the chemical nature of the electrode surface in inducing reversible binding was demonstrated[57] by comparing electrochemistry at the polished 'edge' surface of pyrolytic graphite with that at the freshly-cleaved 'basal plane'. Cytochrome *c* electrochemistry at the hydrophilic edge is well-behaved, but at the hydrophobic basal plane it is essentially irreversible.[57]

[53] A. E. G. Cass, G. Davis, G. D. Francis, H. A. O. Hill, W. J. Aston, I. J. Higgins, E. V. Plotkin, L. D. L. Scott, and A. P. F. Turner, *Anal. Chem.*, 1984, **56**, 667.

[54] J. Lyklema, *Colloids Surf.*, 1984, **10**, 33.

[55] P. M. Allen, H. A. O. Hill, and N. J. Walton, *J. Electroanal. Chem.*, 1984, **178**, 69.

[56] W. J. Albery, M. J. Eddowes, H. A. O. Hill, and A. R. Hillman, *J. Am. Chem. Soc.*, 1981, **103**, 3904.

[57] F. A. Armstrong, H. A. O. Hill, and B. N. Oliver, *J. Chem. Soc., Chem. Commun.*, 1984, 976.

To simulate the redox protein + electrode problem by Brownian dynamics, one might proceed as follows. Assume that the redox protein is spherical (diameter ~ 4 nm) and has two 'patches' on its surface: one for electron transfer (patch P_E), the other for electrostatic binding (P_B). Describe the protein interaction with the surface as a sum of (a) a long-range, centrosymmetric, screened electrostatic interaction and (b) a short-range, specific interaction between protein patch P_B and binding sites S_B on the surface (see Figure 4). Electron transfer is deemed to occur when protein patch P_E gets within some distance δ of the surface. Trajectories can be started with the particle centre at a distance $l = p$ from the surface, and terminated upon reaction or when $l \geqslant q$. The protein model just described can be thought of as a crude representation of, for instance, spinach plastocyanin, a photosynthetic 'blue' copper protein, much of whose net *negative* charge (at neutral pH) is taken to be conservatively localized at the side of the molecule.[58] [By way of contrast, mitochondrial cytochrome *c* has an overall *positive* charge located in close proximity to the electron-transferring haem edge (*i.e.*, for this protein P_B and P_E are coincident).] As far as the surface binding sites are concerned, these could easily represent positively-charged domains of stable chromium(III) complexes, since it has been shown[58] that, even at low background electrolyte concentrations (< 0.01 mol dm^{-3}), a chromium-modified graphite electrode is active towards plastocyanin. A reasonable value for the electron-transfer distance δ probably lies in the range 0.5—1.5 nm.
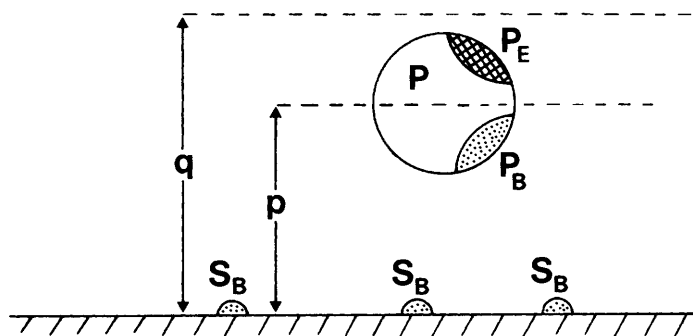

Figure 4 *Representation of spherical redox protein P in vicinity of plane electrode surface with binding sites S_B. The two patches on P are associated with electron transfer (P_E) and specific electrostatic binding (P_B). The distances p and q are equivalent to the same quantities in Figure 3*

As well as giving rate data, a Brownian dynamics simulation along the lines of that described above could be used to determine the importance of translation–rotation coupling effects as the redox protein diffuses at the interface. It is well-known[59–61] that rates of diffusion-controlled biological processes are faster in two dimensions than in three. In diffusion towards a small target of diameter *d* within a

58 F. A. Armstrong, P. A. Cox, H. A. O. Hill, and A. A. Williams, *J. Chem. Soc., Chem. Commun.*, 1985, 1236.

large space of dimensionality n and diameter d_s, Adam and Delbrück have expressed[59] the time to capture as

$$\langle t \rangle = (d_s^2/D)f_n(d_s/d) \qquad (94)$$

where the function $f_n(d_s/d)$ depends on the dimensionality n. For $d_s/d \gg 1$, f_n is linear in d_s/d for $n = 3$; it has the form $\ln(d_s/d)$ for $n = 2$; and it is independent of d_s/d for $n = 1$. So, for a constant diffusion coefficient D, there is a marked enhancement on going from $n = 3$ to $n = 2$, but little change in going from $n = 2$ to $n = 1$. To permit protein motion on a one- or two-dimensional biopolymer surface, the forces between protein and surface must be strong enough to guarantee adsorption, but weak enough to enable the molecule to diffuse. In this connection, small conformational fluctuations may play a role in the sliding of enzymes on the surface of linear or planar biopolymers.[61]

There are clearly similarities between diffusional processes at electrode and membrane surfaces. The electrostatic aspects of redox-protein binding to a negatively charged membrane surface has been demonstrated in a study[62] of the oxidation kinetics of cytochrome c_2 by bacterial photosynthetic reaction centres in unilamellar phosphatidylserine vesicles. In NaCl solution of ionic strength 0.1 mol dm^{-3} or less, the kinetic data suggest that the protein is restricted to the surface of a single vesicle, and encounters reaction centres by two-dimensional diffusion. The retarded oxidation rate at low electrolyte concentrations suggests that electrostatic interaction between the positive haem-cleft face of the protein and the negative membrane is sufficiently strong to restrict protein mobility. With increasing ionic strength, however, mobile counter-ions shield the electrostatic interaction, and so the protein diffuses more rapidly, though still mainly across the surface of the vesicle. Above 0.1 mol dm^{-3} NaCl solution, there is little protein–membrane association, and, since the binding regions are oppositely charged, the reaction rate falls—as it also does in solution, and in neutral phosphatidylcholine vesicles.[62]

The mechanism of protein diffusion at a membrane or electrode surface will depend on the nature of the protein–surface interaction. If the protein is only weakly bound, one would expect a 'hopping' mechanism. With stronger binding, a 'rolling' or 'sliding' mechanism would be more likely, the former being favoured by non-specific electrostatic protein–surface interactions, and the latter by specific interaction with a mobile entity at the interface. From equation 74, we note that the separation between protein and surface must be about one solvent molecule diameter (~ 0.3 nm) or less for there to be appreciable translation–rotation coupling.

C. Antibody Mobility and Antigen Binding.—Animals react adaptively against foreign bodies ('antigens') by synthesizing specific neutralizing agents ('antibodies').

[59] G. Adam and M. Delbrück, in 'Structural Chemistry and Molecular Biology', ed. A. Rich and N. Davidson, Freeman, San Francisco, 1968, p. 198.

[60] F. W. Wiegel and C. DeLisi, *Am. J. Physiol.*, 1982, **243**, R475.

[61] E. Katchalski-Katzir, J. Rishpon, E. Sahar, R. Lamed, and Y. I. Henis, *Biopolymers*, 1985, **24**, 257.

[62] R. E. Overfield and C. A. Wraight, *Biochemistry*, 1980, **19**, 3328.

The commonest class of human antibody is immunoglobulin G (IgG), a Y-shaped glycoprotein (*ca.* 1.5×10^5 daltons) whose structure is illustrated schematically in Figure 5(a). Two identical globular regions known as Fab (after 'fragment antigen binding') are connected flexibly to a third globular region Fc (after 'fragment crystallizable'). It appears that the hinge angle θ can take any value in the range 10—180°. Binding can take place at two separate antigen sites, either on a single particle (bacterium or virus) or on two different ones [see Figure 5(b)]. In terms of protein structure, IgG consists of two equivalent 'light' protein chains ($\sim 2.3 \times 10^4$ daltons) and two equivalent 'heavy' chains ($\sim 5.0 \times 10^4$ daltons) linked by disulphide bridges and non-covalent interactions.[63] Conventionally, the chains are subdivided into variable and constant domains as shown in Figure 5(c). When an antigen binds to the antibody, it nestles in a groove or cleft formed at the contact of the light and heavy chain variable domains. About 10 or so amino-acid residues are thought to be involved in the binding region.[64]
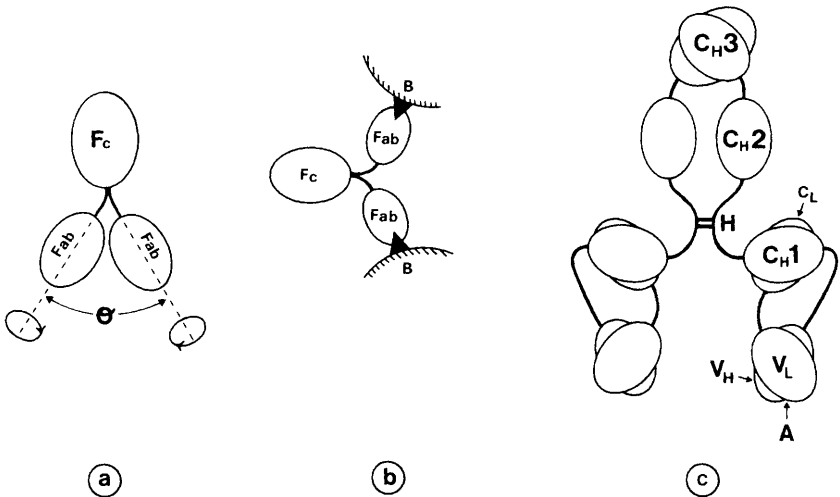

Figure 5 *Representation of the structure of the antibody molecule IgG. (a) Simple three-centre hydrodynamic model. At the hinge, which flexibly connects globular fragment Fc to binding fragments Fab, the angle θ can take up a wide range of values. (b) The binding of IgG to two sites B on different antigen particles. (c) More detailed model showing light (L) and heavy (H) polypeptide chains. The light chain has one constant region (C_L) and one variable region (V_L); the heavy chain has three constant regions (C_H1, C_H2, and C_H3) and one variable region (V_H). The hinge H consists of one or more disulphide interchain bonds. A is the antigen binding site*

Antibody flexibility has been demonstrated experimentally using nanosecond fluorescence spectroscopy.[65,66] A fluorescent chromophore, specifically located at

[63] G. W. Edelman and W. E. Gall, *Ann. Rev. Biochem.*, 1969, **38**, 415.
[64] M. W. Steward, 'Antibodies: Their Structure and Function', Chapman & Hall, London, 1984.
[65] J. Yguerabide, H. F. Epstein, and L. Stryer, *J. Mol. Biol.*, 1970, **51**, 573.
[66] C. L. Lovejoy, D. A. Holowka, and R. E. Cathou, *Biochemistry*, 1977, **16**, 3668.

the antibody binding site, is excited with a short pulse of y-polarized light, and fluorescence intensities polarized in the x- and y-directions, F_x and F_y respectively, are measured as a function of time t. A function

$$A(t) = [F_y(t) - F_x(t)]/[F_y(t) + 2F_x(t)] \qquad (95)$$

expresses how much the orientation of the transition moment has changed between absorption and emission. It was found by Yguerabide *et al.*[65] that $A(t)$ could be approximated as a sum of two exponential terms:

$$A(t) = A_0[f_S \exp(-t/\varphi_S) + f_L \exp(-t/\varphi_L)]. \qquad (96)$$

In equation 96, φ_S and φ_L are short and long rotational correlation times, and A_0, f_S and f_L are constants. Taking $\varphi_S = 33$ ns as the correlation time of an isolated Fab fragment, a fitted value of $\varphi_L = 168$ ns was interpreted as being due to the rotational motion of the antibody molecule as a whole. [An unhydrated rigid sphere with the volume of IgG is estimated to have a rotational correlation time of $\varphi = (6D^R)^{-1} = 44$ ns.] It was inferred[65] that the Fab portions of the intact antibody are free to rotate over an angular range of *ca.* $33°$ in times of nanoseconds. More recently, Lovejoy and co-workers have found[66] similar correlation times, $\varphi_S = 33$ ns and $\varphi_L = 131$ ns, again attributed to Fab segmental flexibility and global antibody rotation, respectively. The flexibility of the IgG molecule is related *inter alia* to the number of disulphide bonds in the hinge region [see Figure 5(c)]. In a comparison of intact and reduced antibodies, it was found[67] that reduction of the inter-heavy-chain disulphide bond increases significantly the internal flexibility of the IgG molecule.

In modelling the IgG molecule as a flexibly connected three-sphere entity [as in Figure 5(a)], torsional interactions between Fab and Fc fragments must be consistent with the above correlation times, which can be computed directly in a Brownian dynamics simulation. The precise structures of antigenic determinants on most protein molecules are not known,[68] but it does appear that interactions normally extend over some 3—4 nm^2 of protein antigen surface. (See the report of an X-ray crystallographic determination[69] of the complex between egg-white lysozyme and the Fab fragment of a monoclonal anti-lysozyme antibody.) In simulating antibody–antigen encounters, as with the enzyme–substrate problem, we can determine how sensitive is the rate constant to such factors as particle size and shape, specific and non-specific electrostatic forces, and so on.

D. Other Protein Diffusional Processes

In biological membranes, various lipids and proteins are able to undergo lateral

[67] L. M. Chan and R. E. Cathou, *J. Mol. Biol.*, 1977, **112**, 653.
[68] D. C. Benjamin, J. A. Berzofsky, I. J. East, F. R. N. Gurd, C. Hannum, S. J. Leach, E. Margoliash, J. G. Michael, A. Miller, E. M. Prager, M. Reichlin, E. E. Sercarz, S. J. Smith-Gill, P. E. Todd, and A. C. Wilson, *Ann. Rev. Immunol.*, 1984, **2**, 67.
[69] A. G. Amit, R. A. Mariuzza, S. E. V. Phillips, and R. J. Poljak, *Nature (London)*, 1985, **313**, 156.

diffusion within the two-dimensional bilayer structure.[70] There are two classes of membrane protein: peripheral and integral. The former associate with membranes predominantly through electrostatic interactions, and their diffusional motion resembles that near a charged electrode surface (*vide supra*). Integral proteins lie partially within the bilayer, where they exhibit extensive hydrophobic and electrostatic interactions with each other and the surrounding lipid molecules.[71] Depending on the conditions, membrane proteins can exist in various states of aggregation. Pair distribution functions derived from freeze-fracture pictures of lipid bilayers resemble[72] those from theoretical models of two-dimensional fluids. Effective protein–protein potentials calculated from experimental pair distribution functions are available[73] for use in simulations.

The function of a membrane appears to be intimately related to its fluidity.[74] In the protein dynamics context, the temperature-dependent viscosity of the bilayer modulates the activity of enzymes and transport-proteins by affecting their lateral and rotational motions. To simulate the Brownian dynamics of membrane proteins, an external potential field could be used to confine the particles to motion in a plane. It would be interesting to compare simulated diffusion coefficients with those measured in fluorescence and phosphorescence decay experiments.[75,76]

Diffusion-controlled encounters occur in a wide range of assembly and polymerization processes involving proteins. An important and well-studied example is the assembly of monomeric G-actin (4.2×10^4 daltons) into polymeric F-actin, a fibrous building block of muscle tissue. The mechanism is supposed to involve a nucleation stage (trimers are the most likely candidates as nuclei), followed by a polymerization stage to give a helical structure.[77,78] Representations of monomeric and polymerized actin suitable for use in a simulation study are illustrated in Figure 6. Bonding between the roughly spherical G-actin molecules occurs through specific interactions of the type a—b and c—d. Solvent conditions sensitively affect the position of the F—G equilibrium,[79] with electrostatic factors particularly important. There is a 'critical' actin concentration for helical polymerization which decreases with increasing ionic strength, reaches a minimum at an optimum ionic strength of 0.1 M NaCl, and then goes up again with further addition of electrolyte. At pH values close to the isoelectric point (pH $\approx$ 4.7), random globular aggregation is superimposed on regular polymerization to F-actin. Divalent cations appear to have both specific and non-specific effects on the

[70] M. D. Houslay and K. K. Stanley, 'Dynamics of Biological Membranes', Wiley, Chichester, 1982.

[71] G. Benga and R. P. Holmes, *Prog. Biophys. Molec. Biol.*, 1984, **43**, 195.

[72] L. T. Pearson, S. I. Chan, B. A. Lewis, and D. M. Engelman, *Biophys. J.*, 1983, **43**, 167; L. T. Pearson, J. Edelman, and S. I. Chan, *Biophys. J.*, 1984, **45**, 863.

[73] J. Naghizadeh, in 'Lecture Notes in Physics No. 172', ed. K.-H. Bennemann, F. Brouers, and D. Quitmann, Springer-Verlag, Berlin, 1982, p. 247.

[74] 'Membrane Fluidity' (Biomembranes, vol. 12), ed. M. Kates and L. A. Manson, Plenum, New York, 1984.

[75] R. Peters and R. J. Cherry, *Proc. Natl. Acad. Sci. USA*, 1982, **79**, 4317.

[76] C. J. Restall, R. E. Dale, E. K. Murray, C. W. Gilbert, and D. Chapman, *Biochemistry*, 1984, **23**, 6765.

[77] F. Oosawa and M. Kasai, in 'Subunits in Biological Systems', ed. S. N. Timasheff and G. D. Fasman, Marcel Dekker, New York, 1971, part A, p. 261.

[78] E. Korn, *Physiol. Rev.*, 1982, **62**, 672.

[79] M. Kasai, S. Asakura, and F. Oosawa, *Biochim. Biophys. Acta*, 1962, **57**, 13.

thermodynamics and the kinetics. At low ionic strengths, G-actin can be polymerized below the critical actin concentration by application of a shear flow field which presumably acts to promote nucleation.[80]
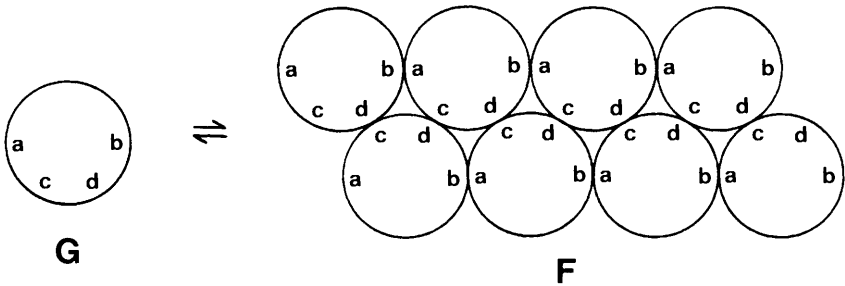

Figure 6 *Equilibrium between monomeric (G) and oligomeric (F) forms of actin. In this model, aggregates are held together by specific attractive interactions of the type a—b and c—d*

Another possible area for Brownian dynamics is in modelling the folding and unfolding of globular proteins.[81,82] Here we have in mind the long-time diffusional motions, rather than the rapid conformational fluctuations.[83,84] That is, the refolding of a denatured protein molecule may be envisaged as the merging of embryo nuclei by a diffusion–collision process. This type of mechanism is consistent with a model[85,86] of a globular protein consisting of hydrophobic clusters loosely connected by covalent bonds, and held in fixed spatial orientations by interacting polar groups on the cluster surfaces. Such a model protein would thermally denature in two stages: an initial phase involving movement of intact clusters relative to one another, followed by a second phase involving disruption of hydrophobic clusters. Co-operativity would come predominantly from the second phase. Also of interest, in addition to thermal denaturation, is protein unfolding at a solid or fluid interface, the kinetics of which is important in the field of food colloids.[87]

7 Simulation of Subunit Models

Complex biological structures can be modelled as a collection of connected subunits. To simulate the dynamics of structures which possess some degree of rigidity, it is necessary to place constraints on the relative motions of different subunits within the total structure. Allison and McCammon have described[88] a

[80] J. Borejdo, A. Muhlrad, S. J. Leibovich, and A. Oplatka, *Biochim. Biophys. Acta*, 1981, **667**, 118.
[81] 'Protein Folding', ed. R. Jaenicke, Elsevier/North-Holland, Amsterdam, 1980.
[82] N. Gō, *Ann. Rev. Biophys. Bioeng.*, 1983, **12**, 183.
[83] R. J. P. Williams, *Biol. Rev.*, 1979, **54**, 389.
[84] CIBA Foundation Symposium No. 93, 'Mobility and Function in Proteins and Nucleic Acids', Pitman, London, 1982.
[85] K. Wüthrich and G. Wagner, *Trends Biochem. Sci.*, 1978, **3**, 227.
[86] K. Wüthrich, H. Roder, and G. Wagner, in *ref.* 81, p. 549.
[87] E. Dickinson and G. Stainsby, 'Colloids in Food', Applied Science, London, 1982.
[88] S. A. Allison and J. A. McCammon, *Biopolymers*, 1984, **23**, 167.

rigorous method of imposing constraints in Brownian dynamics. The procedure is based on the SHAKE molecular dynamics algorithm devised by Ryckaert et al.,[89] and subsequently improved by Ciccotti et al.[90]

In a rigid body of N spherical subunits, $N(N - 1)/2$ inter-subunit distances are invariant. Neglecting gradient terms, the unconstrained Brownian dynamics step is [see equation 78 and note change from scalar to vector notation $(3N \rightarrow N)$]:

$$r_i' = r_i^0 + (\Delta t/kT) \sum_{j=1}^{N} D_{ij}^{to} \cdot F_j^0 + R_i(\Delta t) \quad (i = 1, N) \tag{97}$$

where the prime denotes the new, *unconstrained* co-ordinates of subunit i, and F_j^0 is the total force acting on subunit j, but *excluding* forces of constraint. The corrected co-ordinate r_i is given by

$$\delta r_i = r_i - r_i' = (\Delta t/kT) \sum_{j=1}^{N} D_{ij}^{to} \cdot G_j^0 \tag{98}$$

where G_j^0 is the net force of constraint acting on subunit j. Allison and McCammon have shown[88] that δr_i can be represented as

$$\delta r_i = \sum_{p=1}^{NC} H_{ip}^0 \left[d_{mn}^2 - (r_{mn}')^2 \right] \tag{99}$$

where $r_{mn}' = r_m' - r_n'$, the labels m and n refer to subunits restricted by the pth constraint, d_{mn} is the constrained distance between m and n, NC is the total number of constraints, and

$$H_{ip}^0 = [(D_{im}^{to} - D_{in}^{to}) \cdot r_{mn}^0]/[4r_{mn}^0 \cdot (D_{mm}^{to} - D_{mn}^{to}) \cdot r_{mn}^0] \tag{100}$$

Enforcement of the pth constraint partially destroys those enforced previously. So it is necessary to repeat the cycle of enforcing all constraints until they are satisfied within a specified tolerance level. The procedure reduces to that of Ryckaert et al.[89] in the absence of hydrodynamic interactions, *i.e.* when

$$D_{im}^{to} = D^T \delta_{im} I \tag{101}$$

The Brownian dynamics algorithm with constraints has been tested for an isolated wormlike chain[91] and a pair of rigid cubic octamer particles.[38] The method offers the opportunity for modelling globular proteins and bacterial viruses as multisubunit structures like those described by Garcia de la Torre and Bloomfield.[92,93] Using the above algorithm, we can see how, for instance, a model

[89] J.-P. Ryckaert, G. Ciccotti, and H. J. C. Berendsen, *J. Comput. Phys.*, 1977, **23**, 327.

[90] G. Ciccotti, M. Ferrario, and J.-P. Ryckaert, *Mol. Phys.*, 1982, **47**, 1253.

[91] S. A. Allison and J. A. McCammon, *Biopolymers*, 1984, **23**, 363.

[92] J. Garcia de la Torre and V. A. Bloomfield, *Biopolymers*, 1977, **16**, 1779; 1978, **17**, 1605.

[93] J. Garcia de la Torre and V. A. Bloomfield, *Quart. Rev. Biophys.*, 1981, **14**, 81.

of the antibody–antigen encounter could be successively refined by considering a sequence of multisubunit structures of increasing complexity.

8 Concluding Remarks

Research in colloid science has led to a resurgence of interest in the Brownian motion of small interacting particles.[94] This article has tried to show that the concepts used in colloid science have a broader biological relevance. In particular, from statistical mechanics and fluid mechanics is derived a Brownian dynamics computational algorithm suitable for simulating diffusional processes involving entities like enzymes, immunoglobulins, and redox proteins. A protein is modelled as a single Brownian sphere, or a cluster of connected spheres, and account is taken of electrostatic and other forces to whatever level of complexity is feasible under the circumstances.

The development of reliable electrostatic potentials of mean force between proteins and their subunits is a requirement for substantial progress in this field. The electrostatic interaction between closely approaching proteins can be represented[95] by so-called 'high-dielectric' models, and numerical results of this type have been recently reported by Matthew and co-workers[96] for the putative reaction complex between flavodoxin and ferricytochrome c. Their calculations show that the two molecules begin to become orientated significantly by the electrostatic field at separations closer than *ca.* 0.7 nm, when the interaction free energy is some $2\,kT$ less than the sum of free energies of the isolated molecules. An allowance for electrostatic screening accounts for the experimental increase in flavodoxin–cytochrome c association rate at lower ionic strengths.[97] Cases where electrostatic interactions between protein *subunits* are important include salt bridges in haemoglobin and the superstructure of virus-coat proteins.[98]

Computer experiments are most useful when they can be compared directly with real experiments. Amongst the techniques available for studying colloidal particle motion,[87] quasi-elastic light scattering is particularly useful. It is encouraging to note, therefore, that a recent light-scattering study[99] of aggregating proteins gives information on aggregate structures and rate constants which are suitable for comparing with Brownian dynamics simulations. The techniques of nuclear magnetic resonance[100] and quasi-elastic neutron scattering[101] are also being increasingly applied to protein dynamics, and it seems likely that they will also provide useful data for comparing with the computer simulations, and with analytic theories of the many-body hydrodynamic problem.[102]

[94] E. Dickinson, *Annu. Rep. Prog. Chem., Sect. C*, 1983, **80**, 3.
[95] A. Warshel and S. T. Russell, *Quart. Rev. Biophys.*, 1984, **17**, 283.
[96] J. B. Matthew, P. C. Weber, F. R. Salemme, and F. M. Richards, *Nature (London)*, 1983, **301**, 169.
[97] R. P. Simondsen, P. C. Weber, F. R. Salemme, and G. Tollin, *Biochemistry*, 1982, **21**, 6366.
[98] M. F. Perutz, *Science (New York)*, 1978, **201**, 1187.
[99] J. Feder, T. Jøssang, and E. Rosenqvist, *Phys. Rev. Lett.*, 1984, **53**, 1403.
[100] G. R. Moore, R. G. Ratcliffe, and R. J. P. Williams, *Essays Biochem.*, 1983, **19**, 142.
[101] H. D. Middendorf, *Ann. Rev. Biophys. Bioeng.*, 1984, **13**, 425.
[102] P. Mazur, *Can. J. Phys.*, 1985, **63**, 24.

Appendix

Tensor Multiplication*.—The dot product of tensor T and vector v, in matrix notation, is given by

$$
T{\cdot}v = \begin{bmatrix} T_{11} & T_{12} & T_{13} \\ T_{21} & T_{22} & T_{23} \\ T_{31} & T_{32} & T_{33} \end{bmatrix} \begin{bmatrix} v_1 \\ v_2 \\ v_3 \end{bmatrix} = \begin{bmatrix} T_{11}v_1 + T_{12}v_2 + T_{13}v_3 \\ T_{21}v_1 + T_{22}v_2 + T_{23}v_3 \\ T_{31}v_1 + T_{32}v_2 + T_{33}v_3 \end{bmatrix} = v{\cdot}T\dagger \quad (A1)
$$

where $T\dagger$ is the transpose of T. The dot product is sometimes written more concisely using the summation convention, *i.e.*

$$
(T \cdot v)_k = T_{ki}v_i \tag{A2}
$$

where it is agreed that the indices run from 1 to 3. The inner product of two second-order tensors S and T is itself a second-order tensor:

$$
(S \cdot T)_{ik} = S_{im}T_{mk} \tag{A3}
$$

The double inner product of S and T is given by

$$
S : T = \mathrm{Tr}(S \cdot T) = S_{im}T_{mi} \tag{A4}
$$

where Tr is the trace. The double inner product of a third-order tensor B and a second-order tensor T is a vector:

$$
(B : T)_i = B_{ikm}T_{mk} \qquad (T : B)_i = T_{km}B_{mki} \tag{A5}
$$

The cross product of tensor T and vector v is a tensor:

$$
(T \times v)_{ik} = - T_{ip}\varepsilon_{pkq}v_q \qquad (v \times T)_{ik} = \varepsilon_{ipq}v_p T_{qk} \tag{A6}
$$

In equation A6, ϵ is the Levi-Civita density.

---

* For further details see, for instance, the book 'Cartesian Tensors' (Ellis Horwood, Chichester, 1982) by A. M. Goodbody, from which the nomenclature adopted here was taken. (There is a summary of tensor manipulation, with particular reference to fluid mechanics, in the Appendix to *ref.* 13.)